éclaire
Effects of climate change on air pollution impacts and response strategies for European ecosystems

SEVENTH FRAMEWORK PROGRAMME

Project Number 282910

ÉCLAIRE

Effects of Climate Change on Air Pollution Impacts and Response Strategies for European Ecosystems

Seventh Framework Programme

Theme: Environment

D5.1 Assessment of Current GCMs and CTMS to reproduce recent trends by comparing models and observations

Due date of deliverable: **01/07/2013** Actual submission date: **20/12/2013**

Start Date of Project: **01/10/2011** Duration: **48 months**

Organisation name of lead contractor for this deliverable :
European Commission, Joint Research Centre

Project co-funded by the European Commission within the Seventh Framework Programme		
Dissemination Level		
PU	Public	x
PP	Restricted to other programme participants (including the Commission Services)	☐
RE	Restricted to a group specified by the consortium (including the Commission Services)	☐
CO	Confidential, only for members of the consortium (including the Commission Services)	☐

1. Executive Summary

We present in 5.1.1 trend analysis performed with the LMDz-INCA model, and in 5.1.2 results delivered by TM5, ECHAM5-HAMMOZ, LMDz-INCA-ORCHIDEE, and a host of other models, in the frame of the international ACCMIP and HTAP projects, IPCC AR5, and used for ECLAIRE. Results can be summarized as follows:

- Emission trends of global and regional NOx are qualitatively in agreement with satellite observations with declines in NO2 in North America and Europe in the order of 20-30 % for 1996-2011. There is good qualitative knowledge on decreases of precursor gases CO and NMVOC in Europe and the US.
- Deposition trends in Europe are reasonably well understood by global and regional models, transport of reactive nitrogen from outside Europe may contribute by 5-10% to deposition in Europe.
- Trend of inflow of ozone at Europe's boundary is only partly understood: attribution of changes typically can explain up to half the observed changes. Possible explanations include important roles of decadal scale variability, and possibly missing information on long-range transport of anthropogenic pollution. Scaling of regional boundary conditions with observations at Mace Head provides an accurate assessment of Europe-wide changes, but may be problematic for future conditions.

2. Objectives:

To assess our current understanding of ozone and other air pollution trends, based on knowledge acquired within the UNECE TF HTAP, work for IPCC-AR5 and other projects, with a focus on the inflow regions of Europe.

3. Activities:

Global Modelling with ECLAIRE models, and participation in and contribution to global modelling projects.

4. Results:

4.1 Trend analysis with the LMDz-INCA model

The LMDz-INCA-ORCHIDEE global chemistry-aerosol-climate model couples on-line the LMDz (**L**aboratoire de **M**étéorologie **D**ynamique, version 4) General Circulation Model, the INCA (**IN**teraction with **C**hemistry and **A**erosols, version 3) chemistry model and ORCHIDEE (**OR**ganizing **C**arbon and **H**ydrology **I**n **D**ynamic **E**cosyst**e**ms) version 9 dynamical vegetation model.

In the framework of ECLAIRE a new version of the model has been developed to include the NH_3 cycle and the ammonium nitrate and ammonium sulfate particles. A description of the model components is given in (Hauglustaine et al., 2013). Hindcast simulations for the period 1960, 1970, 1980, 1990, and 2000, have been performed, using ECMWF meteorology for the years 2005-2006, and anthropogenic emissions from Lamarque et al. (2010). The monthly mean results from the LMDz-INCA global model to be used as boundary conditions for regional scale models within ECLAIRE are available as NetCDF files (see also D.5.4)

In order to illustrate the model results and investigate the role played by anthropogenic emissions on the evolution of atmospheric composition, Figure 5.1.1 shows the **CO summer surface mixing ratio** for the year 1960, 1970, 1980 and 2000. Due to increasing emissions, CO mixing ratio has increased over the considered period up to 1990 in the northern hemisphere and in Europe in particular, with summer mixing ratios reaching more than 150 ppbv over most of Europe and up to 300 ppbv in northern Europe in 1980. Due to decreasing emissions after 1990, the summer time surface mixing ratio has decreased below 200 ppbv in 2000. Despite the shorter CO lifetime in summer due to its oxidation by OH, the simulations also show an increase in background CO with mixing ratio increasing over the Northern Atlantic from maximum values of 70-80 ppbv in the 1960s up to 90-100 ppbv in the 1980s.

Figure D5.1.1. Distribution of CO surface mixing ratio (ppbv) calculated for JJA conditions and for the year 1960, 1970, 1980, and 2000.

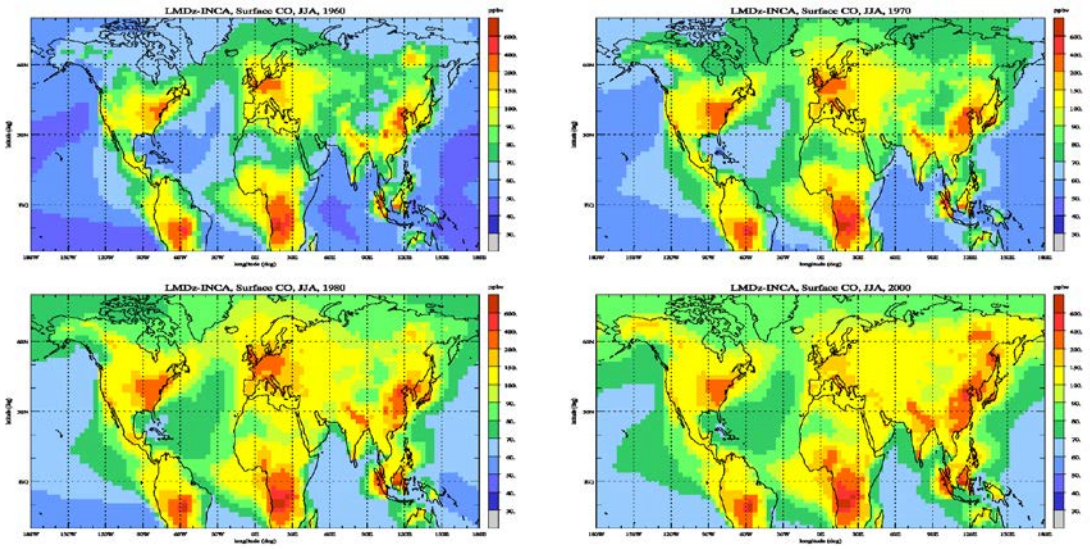

Figure 5.1.2 illustrates the evolution of the surface ozone mixing ratio for JJA conditions over 1960-2000. The simulated ozone mixing ratio increased from 40-45 ppbv over Western Europe in 1960 to values reaching 45-50 ppbv in Northern Europe with marked maximum values in Southern and Central Europe reaching 55 ppbv in Spain, Italy, Greece, and the South of France in 1980 (and 1990, not shown). Due to decreasing emissions of ozone precursors in the emission inventories, the O_3 surface mixing ratios have started to decrease after 1990 with maximum values of 50-55 ppbv still confined in the Mediterranean basin but with mixing ratios decreased by 5-10 ppbv in Northern Europe. Over the Northern Atlantic, the ozone background concentration increased from 20-25 ppbv in 1960 up to 25-30 ppb at the end of the 20th century.

Figure D5.1.2. Distribution of O_3 surface mixing ratio (ppbv) calculated for JJA conditions and for the year 1960, 1970, 1980, and 2000.

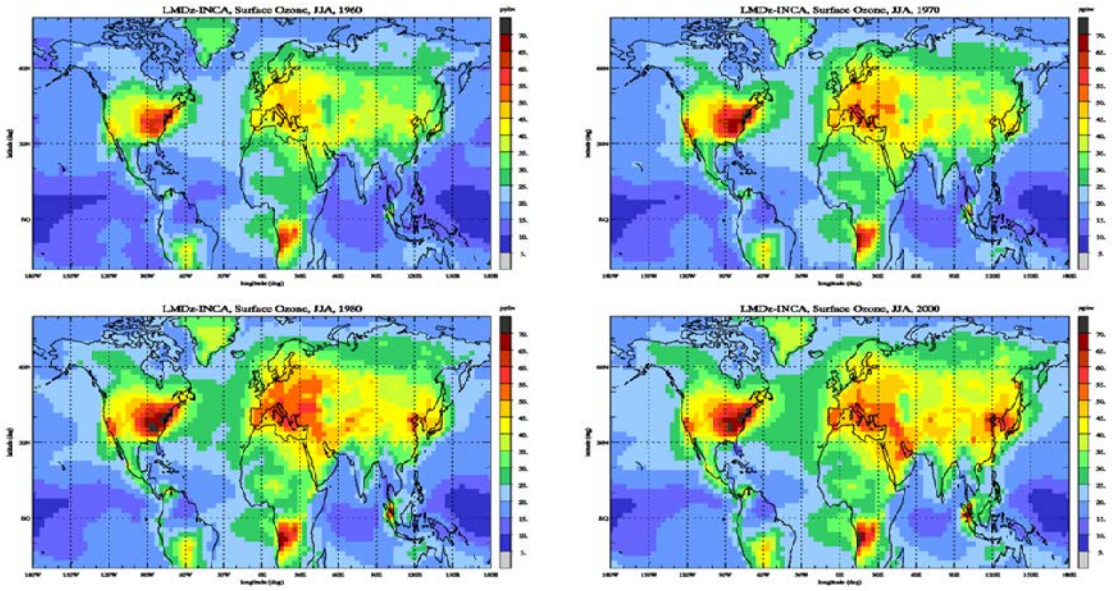

Nitrogen and sulphur deposition over the 1960-2000 period are evaluated in Figure 5.1.3 showing the comparison of the model simulated deposition of SO_4, total NH_x (=NH_3+NH_4^+), and total NO_y compared to measurements in Europe for present day condition. Overall a good agreement is reached for the three parameters considering the difficulty to reproduce these measurements with a global model with coarse resolution. As shown on these plots the wet deposition for sulphates and total NO_y is underestimated by about 25%. For total NH_x a better agreement is reached and the measurements are underestimated by only 4.5%. Similar patterns have been obtained over Northern America (IMPROVE network) and over Asia (EANET network).

Figure D5. 1.3. Model-measurement comparison for SO_4, NH_x, and NO_y wet deposition over Europe (gN-S/m2/yr).

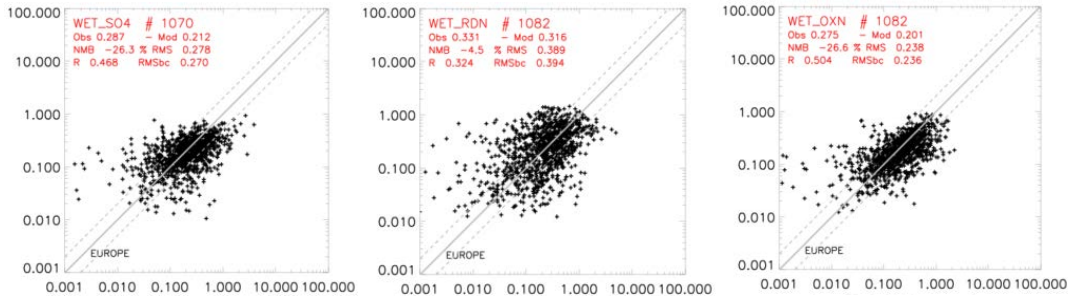

Figure 5.1.4 shows the evolution SO_4, total NH_x, and total NO_y dry+wet surface deposition from 1960 to 2000 as simulated by the model. Decreased SO_2 emissions had a significant impact on SO_4 deposition over the 40 year period. Over Europe in particular, sulphate deposition decreased from values reaching more than 800-900 mgS/m^2/yr in 1960 to values generally lower than 300 mgS/m^2/yr in 2000 in Western Europe. In 2000, maximum values of about 400 mgS/m^2/yr are calculated in Central Europe. In contrast the sulphate deposition has significantly increased over China reaching more than 800 mgS/m^2/yr in 2000. Increase in NH_3 and NO_x emissions is responsible for a significant increase in NH_x deposition in the central US, in Europe and to an even larger extent in South East Asia and India. In Northern Europe in particular, the total NH_x deposition increased from 600 mgN/m^2/yr in 1960 up to 1 gN/m^2/yr in 2000 in the Benelux and Northern France. Total NO_y also increased over the considered period but to a much lesser extent than NH_x in Europe. Maximum values of annual mean deposition of 800 mgN/m^2/yr are reached in Northern Europe in 2000. Over China and India, the total NO_y reaches more than 1 gN/m^2/yr in several areas.

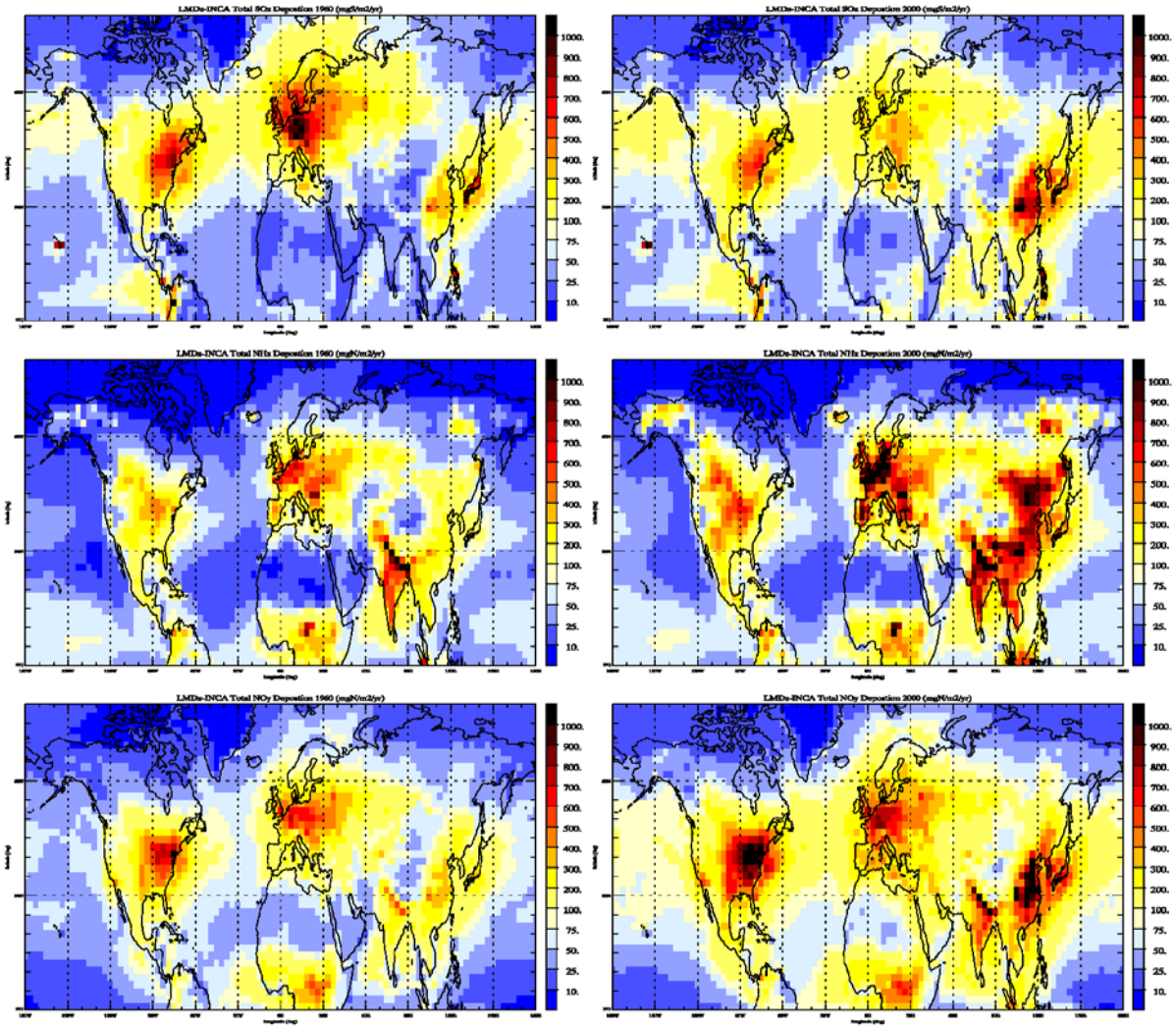

Figure D5.1.4. Annual mean total surface deposition of (top row) SO_4 (mgS/m^2/yr), (middle) total NH_x and (bottom) total NO_y (mgN/m^2/yr) calculated in 1960 (left) and in 2000 (right).

4.2 Trends analysed in HTAP, ACCMIP and IPCC-AR5

The global models participating in ECLAIRE (including LMDZ-INCA and TM5) have been contributing to community analysis of air pollution trends over the past decades-to-century timescales.

Here results from ACCMIP (Atmospheric Chemistry and Climate Model Intercomparison Project), HTAP and ECHAM5-HAMMOZ are synthesized and summarized.

5.1.2.1 Ozone trends

Figure 5.1.5 shows a comparison of a multi-model current day ozone climatology radio-sonde and TES satellite observations, produced within ACCMIP (Young et al., 2013). Overall current day remote ozone is accurately described by current models, with the exception of upper tropospheric ozone, which is biased low.

Figure D5.1.5. Ability of current models to reproduce tropospheric ozone current-day background climatology (Young et al. 2013)

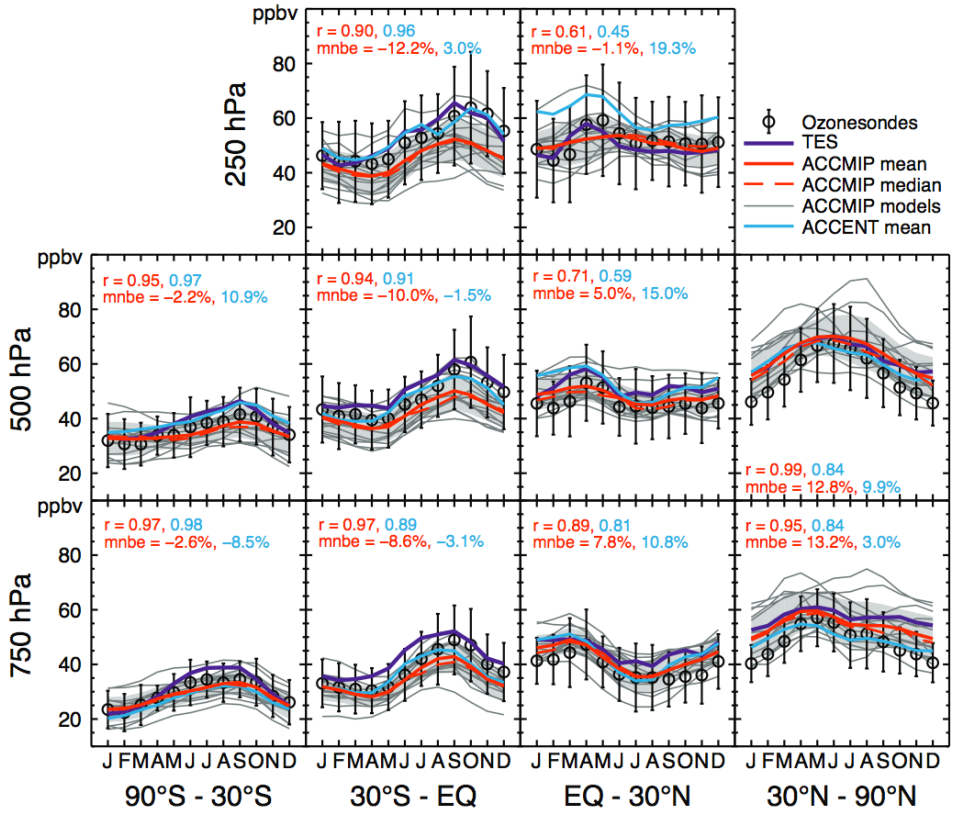

Lamarque et al. (2010) (Figure 5.1.6) performed a comparison of timeseries (1960-2009) of a subset of two models (Figure 2.1.6). Of the linear trends fro 1960-2009 trends at the South Pole, Samoa, Mauna Loa, Barrow are reproduced with an error of ±0.1 ppb/yr. Mace Head unfiltered data are accurately reproduced at 0.17 ppbv/yr (since 1989); whereas trends at Hohenpeissenberg, Zugspitze and Arkona are lower by a factor 2 or 3 compared to the observations (ca. 0.3 to 0.4 ppb/yr), although individual models were substantially biased compared to the observations.

Figure D5.1.6 Ozone trends at 4 stations by the GISS and CAM-Chem models, a subset of models in ACCMIP (Lamarque et al.; 2010). Zugspitze, Mace Head and Arkona are situated in Europe.

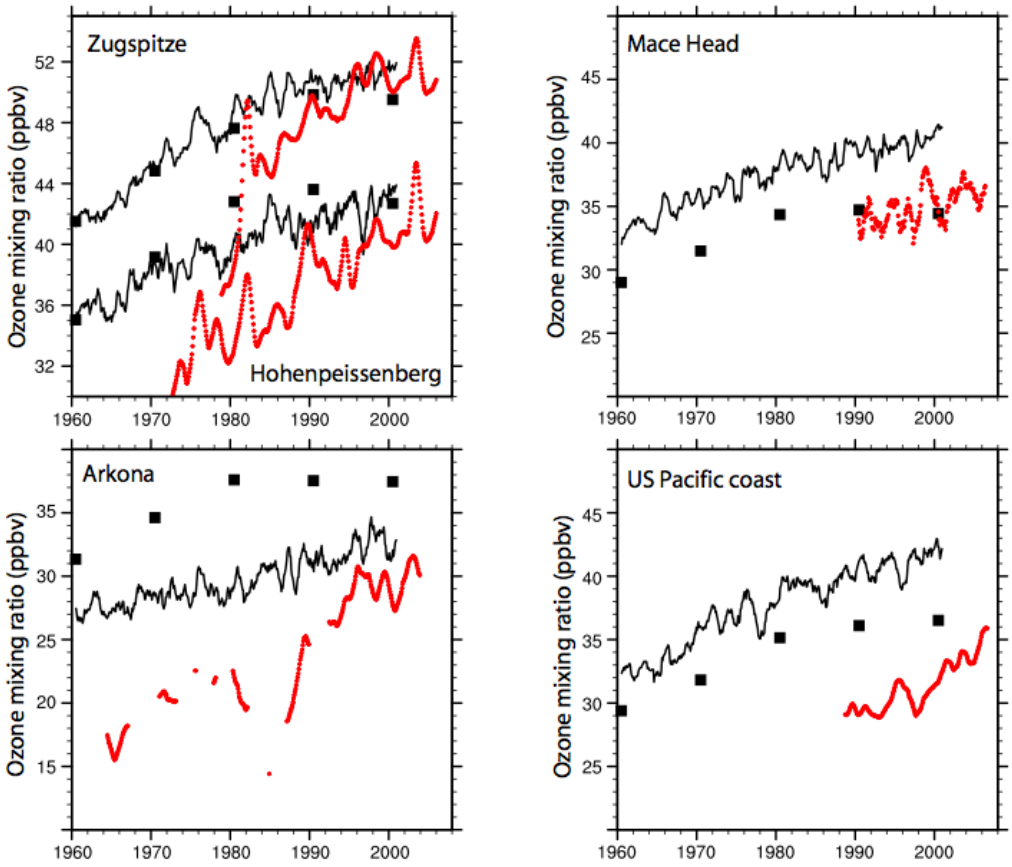

Using results from HTAP (2010), Wild et al. (2012; 2013) analysed these decadal trends with respect to source contributions from Europe, North America, South and East Asia, the Rest-of-the-World (representing ca. 40 % of the global NOx sources) and CH4. A more detailed analysis by Wild et al. (2013), using an ensemble of HTAP model sensitivity simulations, shows that using the best assessment of past emission changes models underestimate recent ozone trend at at the western boundary of Europe as wells as remote continental sites in Europe, and show a turnover in ozone a decade earlier than observed.

Figure D5.1.7 Ozone changes attribution to World Regions for the last decades showing trends from 1960-2000 for North America, Europe, South and East Asia. Lower panels give attribution to regional source, extra-regional and global Methane sources.

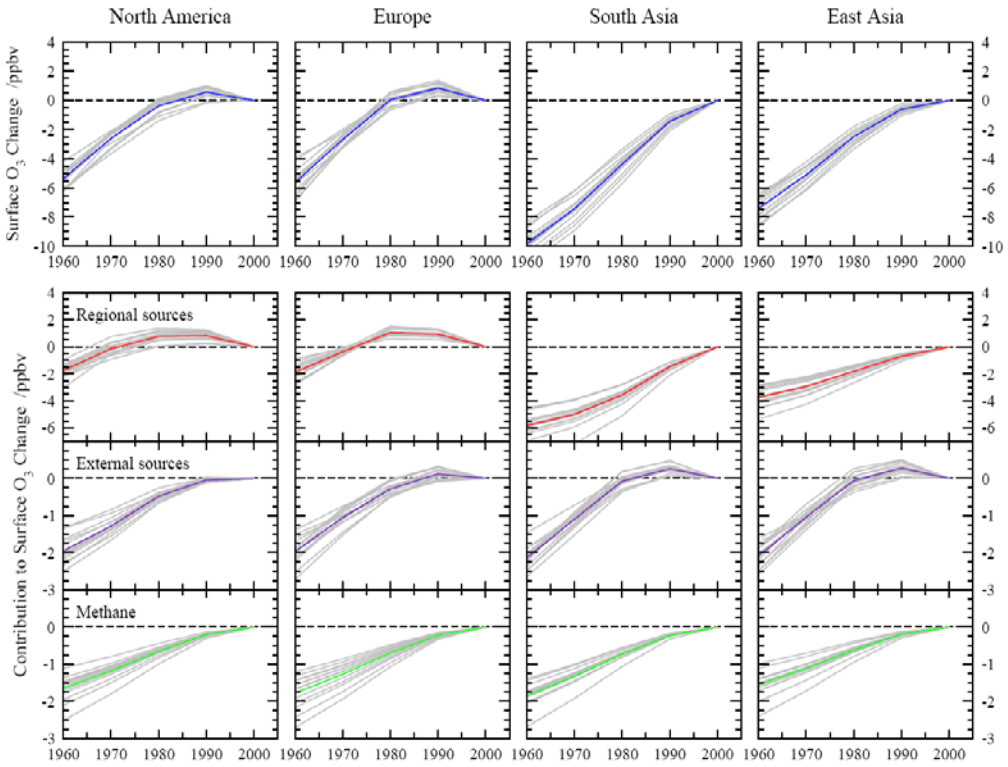

Using the ECHAM5-HAMMOZ model, Pausata et al. (2012) show a strong relationship between the NAO-index and O3 variability at Mace Head, as well over continental Europe (Figure 5.1.8). Their analysis of recent trends at Mace Head, suggest that the recent slow-down of O3 increases at Mace Head is at least partly attributable to decadal scale meteorological variability as represented in NAO index.

Figure D5.1.8 Seasonal and annual observed and modelled ozone variations at Mace Head and correlation with NAOI (PCI1). PC1 principal component 1 is an indicator of NAO.

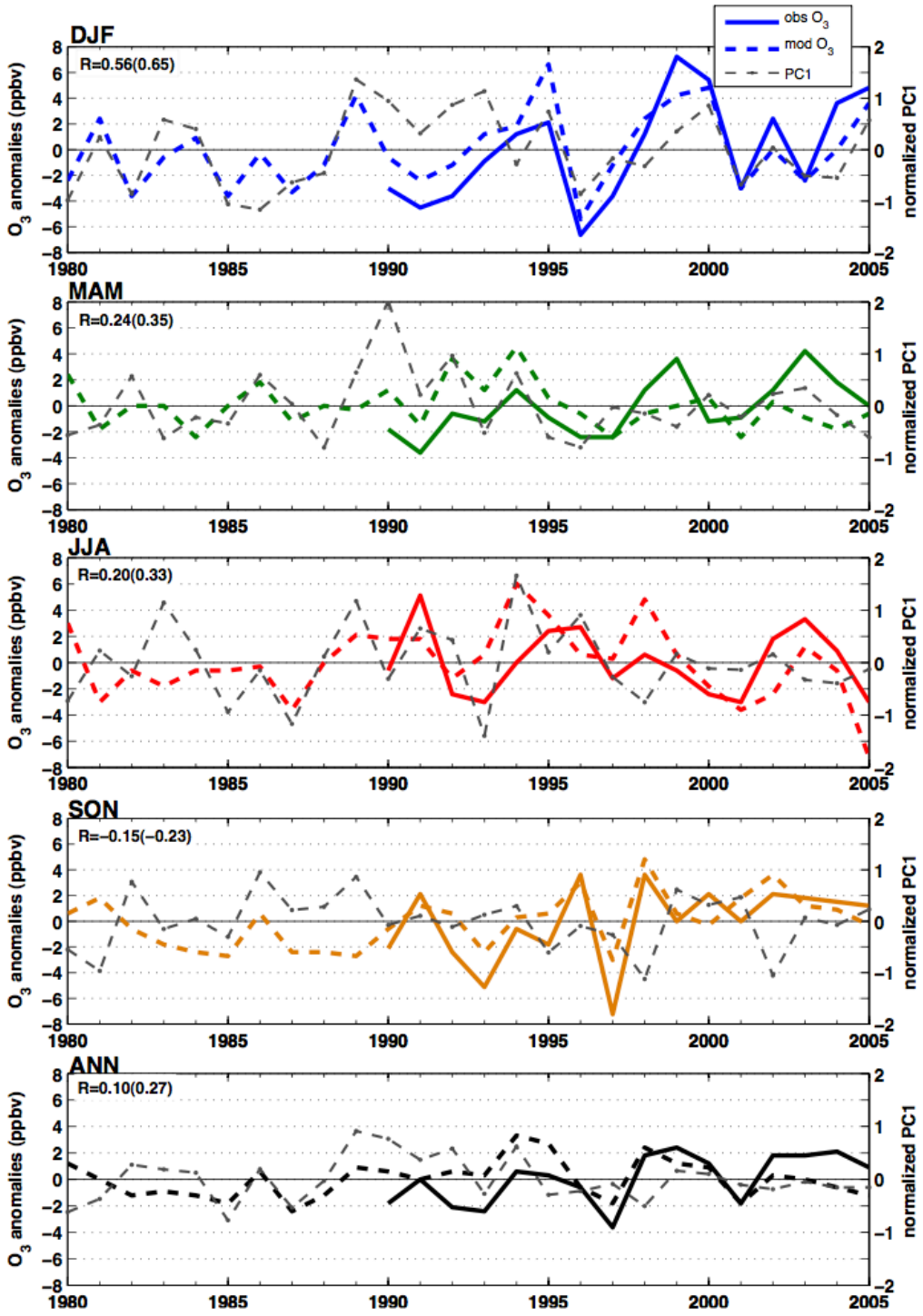

4.2.2 NO2 trends

The most recent assessment of satellite observed regional/world NO_2 trends was presented by Hilboll et al. (2013) and input to IPCC AR5. Satellite and surface observations of ozone precursor gases NO_x, CO, and non-methane volatile organic carbons indicate strong regional differences in trends (Figure 5.9) Most notably NO_2 has *likely* decreased by 30-50% in Europe and North America and increased by more than a factor of 2 in Asia

since the mid-1990s. Regional model analysis, e.g. using the Asian REAS inventory, indicated that Asian emissions reasonably reproduced the annual trends observed by multi-satellites, suggesting that the NO_x emissions growth rate estimated by the updated REAS is robust. Figure 5.9 shows the changes relative to 1996 in satellite derived tropospheric NO_2 columns, with a strong upward trend over central eastern China and an overall downward trend in Japan, Europe and the USA. NO_2 reductions in the USA are very pronounced after 2004, related to differences in effectiveness of NO_x emission abatements in the USA and also to changes in atmospheric chemistry of NO_x. Increasingly, satellite data are used to derive trends in anthropogenic NO_x emissions, with overall increases in global emissions, driven by Asian emission increases of up to 29%/yr (1996–2006), while moderate decreases up to 7%/yr (1996–2006) are reported for North America and Europe. A comparison with regional JRC EDGAR4.2 Emission inventory indicates consistent trends for Europe, India and the US, but potentially an underestimate in the emissions (in 2008 an increase by a factor of 1.8 in EDGAR4.2 and 2.3 in the observations). Note however, that in this preliminary analysis the region extents were not matching.

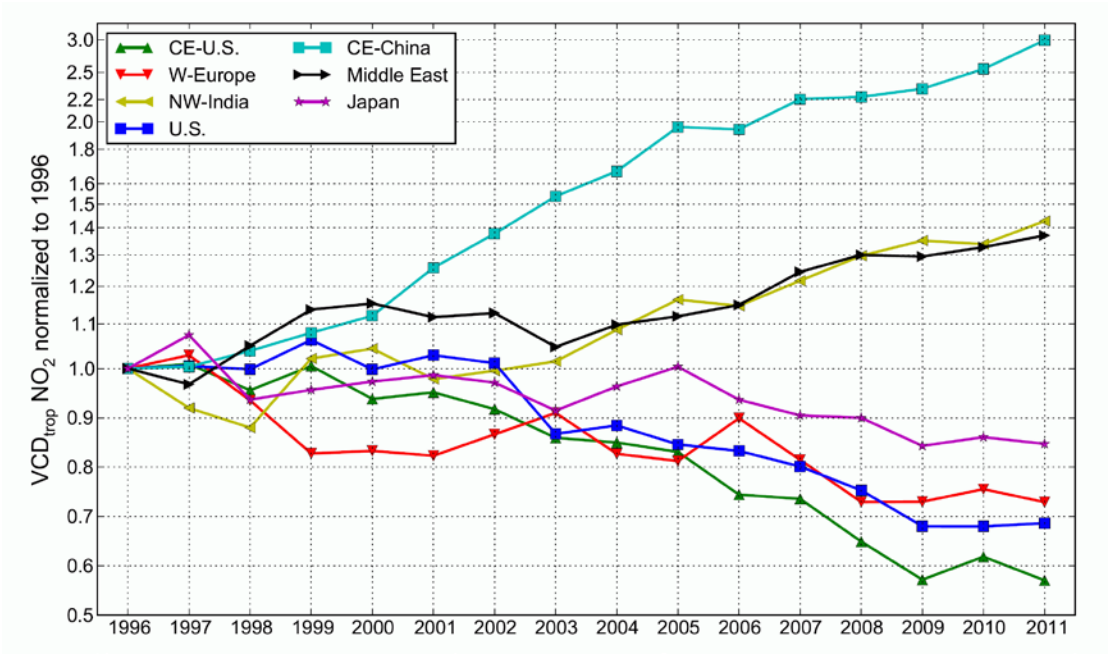

Figure 5.1.9:

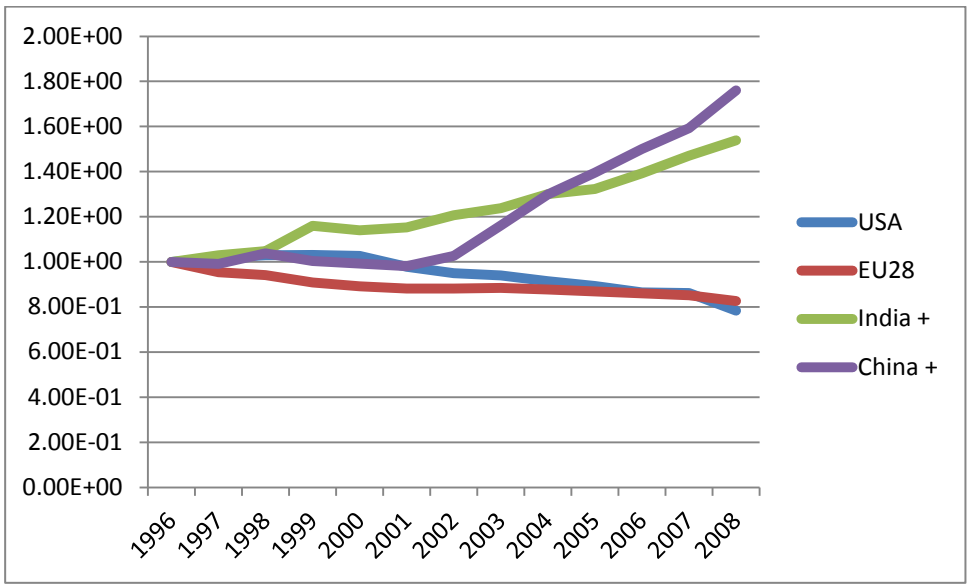

Figure D5. 1.10 EDGAR4.2 NOx emission trends; http://edgar.jrc.ec.europa.eu/index.php

4.2.3 Aerosol trends

Rural PM10, PM2.5 and sulphate aerosol trends in the US and Europe were summarized by IPCC-AR5 and shown in Figure 5.1.11. Trends are around -1 to -5 % at a number of rural sites in North America and the US, but a large interannual variability precludes making robust statistical statements at many sites as well.

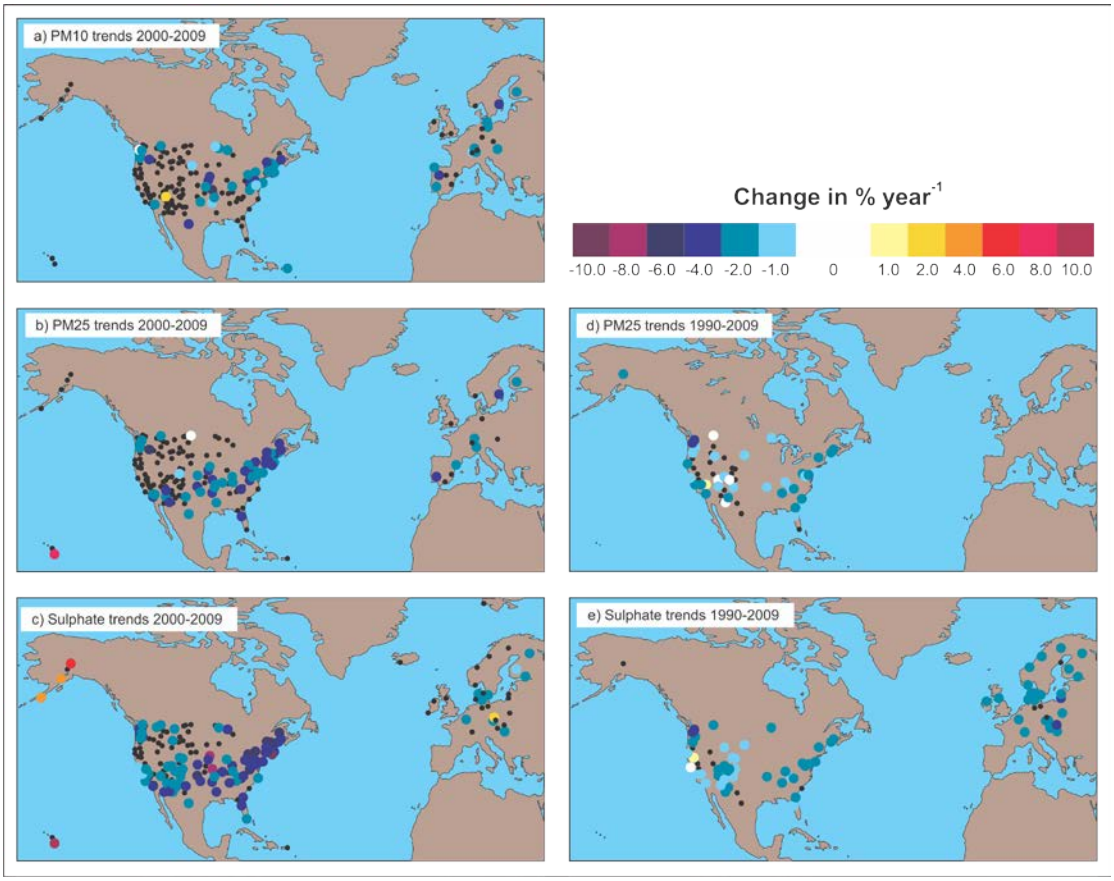

Figure D5.1.11 Trends in particulate matter (PM_{10} and $PM_{2.5}$ with aerodynamic diameters < 10 and 2.5 µm, respectively) and sulphate in Europe and USA for two overlapping periods 2000-2009 (a, b, c) and 1990-2009 (d, e). The trends are based on measurements from the EMEP and IMPROVE networks in Europe and USA, respectively. Sites with significant trends (i.e. a trend of zero lies outside the 95% confidence interval) are shown in colour; black dots indicate sites with non-significant trends. Figure from Chapter 2 of IPCC AR5 WG report (IPCC,Chapter 2, 2013)

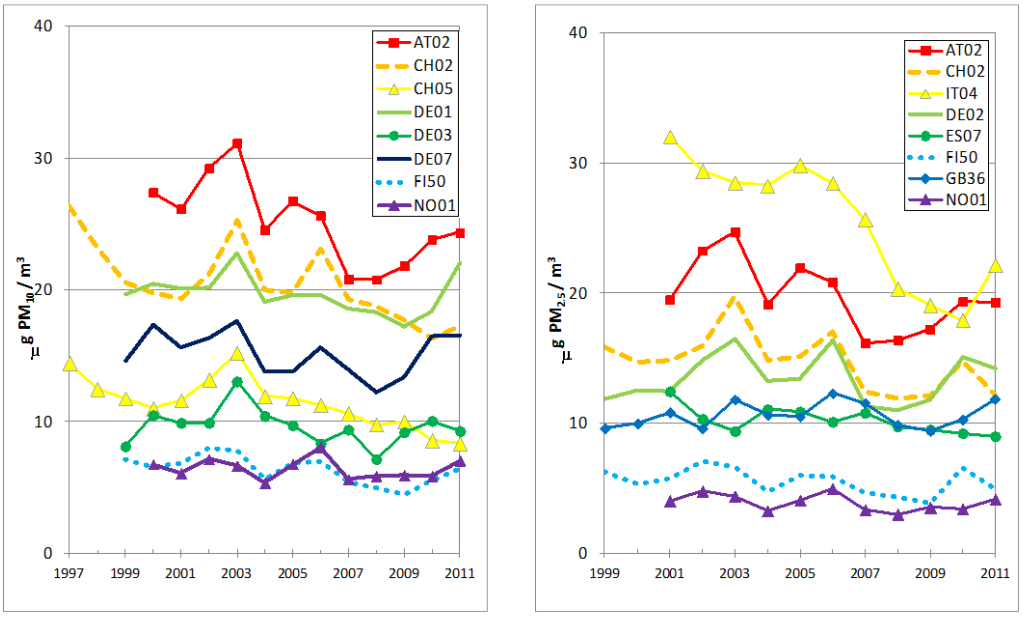

D5.1.12 Time series from 1997 (1999) to 2011 of PM_{10} (left) and $PM_{2.5}$ (right) at selected EMEP sites. EMEP

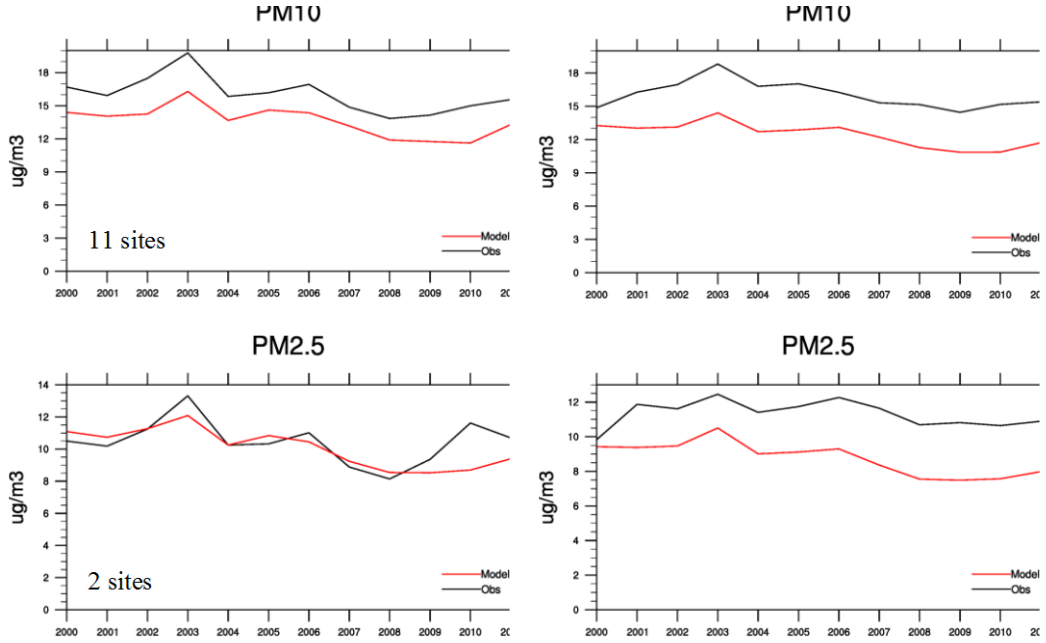

Figure 5.1.13: Calculated and observed 12-year time series in annual mean PM_{10} and $PM_{2.5}$ concentrations from 2000 to 2011: left – only for the EMEP sites with measurements during the whole 12-year period; right – all EMEP sites with PM measurements.

For the period 2005-2011, the EMEP model (EMEP, report 2013) finds a good agreement between modelled and observed PM trends (with the model underestimating by 18-20% the measured PM). For both PM_{10} and $PM_{2.5}$, the mean concentrations drop from 2006 to 2008-09 and then somewhat increase to 2010-11.

These declines are further corroborated by satellite observations: IPCC, AR5 states that it is *very likely* that aerosol column amounts have declined over Europe and the eastern USA since the mid 1990s and increased over eastern and southern Asia since 2000.

Nitrogen and Sulphur Deposition

Hauglustaine et al. (2013) showed an overall good comparison of model results in comparison to wet deposition measurements in North America and Europe. Using the same emission data but an extended set of models participating in the ACCMIP exercicse, Lamarque et al. (2013) showed a similar skill of a set of global models over North America/Europe, but deteriorated skills, especially over North America to understand trends between 1980-2000. These were attributed to uncertainties to capture North American emission changes in the dataset summarized by Lamarque et al. (2010). HTAP (2010) reported source receptor relationships for 4 major Northern Hemispheric regions. Overall in the order of 5-10 % of reactive Nitrogen deposited over Europe was evaluated to originate from Non-European sources.

Figure 5.1.14 Sanderson (2008) evaluation of long-range impact of reactive nitrogen deposition arriving in Europe as in HTAP 2010 report.

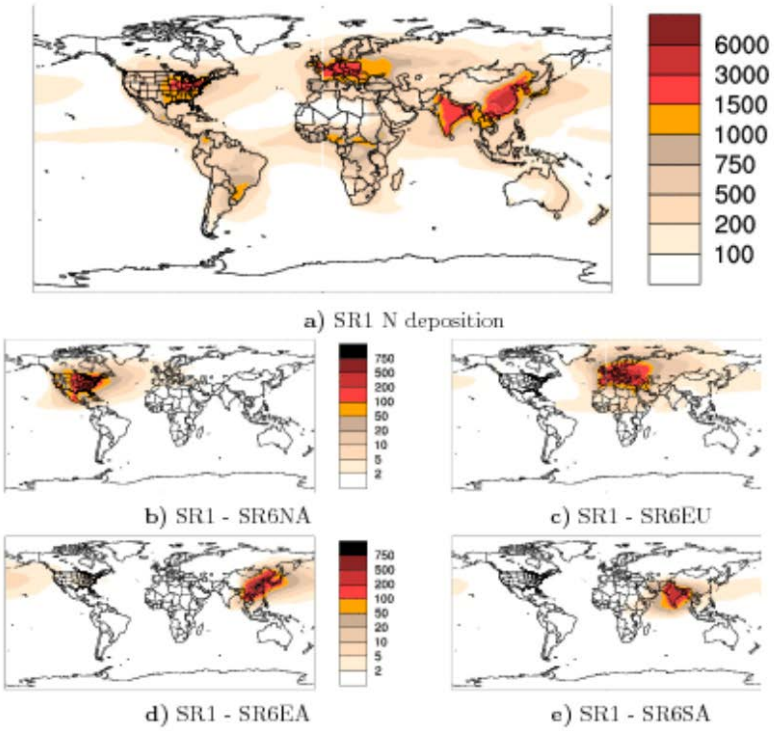

5. Milestones achieved:

Evaluation of AR5 and other simulations with climate and chemistry global models (month 18) partly achieved in month 18 and fully achieved in Month 24.

6. Deviations and reasons:

D5.1 was delivered with a delay of about six months. The reasons were:
Change of supercomputer at CNRS caused half a year of delay. Delay of about half a year of community analysis for the Task Force Hemispheric Transport. No major impact expected.

7. Publications:

Hauglustaine, D. A., Y. Balkanski, and M. Schulz, A global model simulation of present and future nitrate aerosols and their direct radiative forcing of climate, submitted to *Atmospheric Chemistry and Physics*, 2013.

Hilboll, A., Richter, A. and Burrows, J.P., 2013. Long-term changes of tropospheric NO2 over megacities derived from multiple satellite instruments. Atmos. Chem. Phys., 4145-4169, 2013.

IPCC, 2013: Chapter 2, *Climate Change 2013: The Physical Science Basis. Contribution of Working Group I to the Fifth Assessment Report of the Intergovernmental Panel on Climate Change* [Stocker, T.F., D. Qin, G.-K. Plattner, M. Tignor, S. K. Allen, J. Boschung, A. Nauels, Y. Xia, V. Bex and P.M. Midgley (eds.)]. Cambridge University Press, Cambridge, United Kingdom and New York, NY, USA.

Lamarque J.-F., T. C. Bond, V. Eyring, C. Granier, A. Heil, Z. Klimont, D. Lee, C. Liousse, A. Mieville, B. Owen, M. G. Schultz, D. Shindell, S. J. Smith, E. Stehfest, J. Van Aardenne, O. R. Cooper, M. Kainuma, N. Mahowald, J. R. McConnell, V. Naik, K. Riahi, and D. P. van Vuuren, Historical (1850–2000) gridded anthropogenic and biomass burning emissions of reactive gases and aerosols: methodology and application, Atmos. Chem. Phys., 10, 7017-7039, 2010.

Lamarque, J.-F., Dentener, F., McConnell, J., Ro, C.-U., Shaw, M., Vet, R., Bergmann, D., Cameron-Smith, P., Dalsoren, S., Doherty, R., Faluvegi, G., Ghan, S. J., Josse, B., Lee, Y. H., MacKenzie, I. A., Plummer, D., Shindell, D. T., Skeie, R. B., Stevenson, D. S., Strode, S., Zeng, G., Curran, M., Dahl-Jensen, D., Das, S., Fritzsche, D., and Nolan, M.: Multi-model mean nitrogen and sulfur deposition from the Atmospheric Chemistry and Climate Model Intercomparison Project (ACCMIP): evaluation of historical and projected future changes, Atmos. Chem. Phys., 13, 7997-8018, doi:10.5194/acp-13-7997-2013, 2013.

Pausata, F. S. R. , L. Pozzoli, E. Vignati and F. J. Dentener, North Atlantic Oscillation and tropospheric ozone variability in Europe: model analysis and measurements intercomparison, Atmospheric Chemistry and Physics, 12, 6357–6376, 2012.

M.G. Sanderson, F.J. Dentener, A.M. Fiore, C. Cuvelier, T.J. Keating, A. Zuber, C.S. Atherton, D.J. Bergmann, T. Diehl, R.M. Doherty, B.N. Duncan, P. Hess, L.W. Horowitz, D. Jacob, J.-E. Jonson , J.W. Kaminski, A. Lupu, I.A. Mackenzie, E. Marmer, V. Montanaro, R. Park, G. Pitari, M.J. Prather, K.J. Pringle, S. Schroeder, M.G. Schultz, D.T. Shindell, S. Szopa, O. Wild, P. Wind: A multi-model source-receptor study of the hemispheric transport and deposition of oxidised nitrogen, 35, L17815, doi:10.1029/2008GL035389, 2008.

Young, P. J., A. T. Archibald, K. W. Bowman, J.-F. Lamarque, V. Naik, D. S. Stevenson, S. Tilmes, A. Voulgarakis, O. Wild, D. Bergmann, P. Cameron-Smith, I. Cionni, W. J. Collins, S. B. Dalsøren, R. M. Doherty, V. Eyring, G. Faluvegi, L. W. Horowitz, B. Josse, Y. H. Lee, I. A. MacKenzie, T. Nagashima, D. A. Plummer, M. Righi, S. T. Rumbold, R. B. Skeie, D. T. Shindell, S. A. Strode, K. Sudo, S. Szopa, and G. Zeng, Pre-industrial to end 21st century projections of tropospheric ozone from the Atmospheric Chemistry and Climate Model Intercomparison Project (ACCMIP), Atmos. Chem. Phys., 13, 2063-2090, 2013.

Wild, O., F.J. Dentener, K.S. Law, J.E. Jonson, V.S. Semeena, C. Andersson, D.D. Parrish, and M. Amann, Changing ozone at Europe's borders: present-day and future perspectives for air quality, to be submitted to ACP, 2013.

Wild, O., A.M. Fiore, D.T. Shindell, R.M. Doherty, W.J. Collins, F.J. Dentener, M.G. Schultz, S. Gong, I. A. MacKenzie, G. Zeng, P. Hess, B.N. Duncan, D.J. Bergmann, S. Szopa, J.E. Jonson, T.J. Keating, and A. Zuber, Future Changes in Surface Ozone: A Parameterized Approach, Atmos. Chem. Physics, 12, 2037–2054, 2012.

8. Meetings:

Participation in ECLAIRE plenary meetings.

9. List of Documents/Annexes:

None.